

PACS numbers: 42.65.Ky; 42.55.Vc; 32.80.Fb
DOI: 10.1070/QE2013v043n03ABEH015098

On the potential of mid-IR lasers for generating high harmonics with subnanometer wavelengths in gases

M.Yu. Emelin, M.Yu. Ryabikin

Abstract. **The influence of the magnetic field of a laser pulse and the depletion of bound levels of working-medium atoms on the generation of high harmonics of mid-IR laser radiation in gases is investigated using numerical quantum-mechanical calculations. The maximum attainable spectral widths of high harmonics are estimated for model atoms with different ionisation potentials taking into account the aforementioned limiting effects. It is shown (within a two-dimensional model) that high harmonics with wavelengths to several angstroms can be generated by irradiating helium atoms with high-power femtosecond pulses of a laser [5] with a centre wavelength of 3.9 μm. The possibility of observing experimentally relativistic effects using modern desktop mid-IR laser sources is demonstrated.**

Keywords: *mid-IR lasers, atoms, ionisation, high-harmonic generation, X rays, relativistic effects.*

1. Introduction

Until recently, the main experimental tool in physics of superstrong light fields was the Ti:sapphire laser – a source of high-power femtosecond radiation with a centre wavelength near 800 nm. However, significant progress has been achieved in the development of high-power femtosecond parametric near- and mid-IR laser sources in the last few years. Sources of different types have been designed, which generate ultrashort (few-cycle) pulses with a pulse energy on the order or more than 1 mJ; their working wavelengths are in the range from 1.5 to 4 μm [1–6]. The development of these sources opens new ways to study the interaction of high-intensity laser radiation with matter [7].

An important characteristic of various processes related to ionisation of gases by intense laser radiation is the average energy of electron oscillations in an ac electric field with an amplitude E and a frequency ω (ponderomotive energy):

$$U_\mathrm{p} = \frac{e^2E^2}{4m\omega^2} \sim I\lambda^2, \tag{1}$$

where e is the elementary charge, m is the electron mass, I is the laser radiation intensity, and λ is the lasing wavelength. The U_p value determines, in particular, the energy characteristics of the free electrons and photons generated at tunnel ionisation of atoms and molecules. In particular, the position of the high-energy edge of the plateau-like distribution [8, 9] in the spectrum of high-order harmonic generation (HHG) in gases is determined by the universal expression [10, 11]

$$\hbar\Omega_\mathrm{max} \approx I_\mathrm{i} + 3.17U_\mathrm{p}, \tag{2}$$

where I_i is the atomic ionisation potential, and the high-energy cutoff in the spectrum of free electrons at high-order above-threshold ionisation is given by [12, 13]

$$E^\mathrm{e}_\mathrm{max} \approx 10U_\mathrm{p}. \tag{3}$$

The proportionality of the ponderomotive electron energy to the squared laser wavelength (1) is one the most important factors determining the advantages of long-wavelength sources in generation of high-energy photons and electrons. This feature, in particular, makes it possible to expand significantly the plateau in the HHG spectrum to higher frequencies, which was experimentally demonstrated for the first time in [14]. According to (1), the input intensity can be taken even lower than in the case of a shorter-wavelength source. This circumstance is attractive for reducing the undesirable influence of the effects that are related to intense gas ionisation and lead both to a decrease in the number of neutral atoms involved in generation of harmonics and to a phase mismatch of atomic oscillators and laser beam defocusing due to the increase in the plasma density.

In turn, easier achievement of phase matching in a macroscopic volume of a gas medium using long-wavelength sources [15, 16] allows one to operate with denser gases and, correspondingly, significantly compensate for the fast decrease (proportional to $\lambda^{-5} - \lambda^{-6}$ [17–19]) in the efficiency of harmonic generation by individual atoms with an increase in λ. This approach was successfully demonstrated in the recent experiment [20], where HHG of high-power femtosecond pulsed radiation [5] with a centre wavelength of 3.9 μm, interacting with helium atoms in a capillary at a high (to 35 atm) pressure, was used to obtain a coherent broadband supercontinuum with a maximum photon energy up to 1.6 keV. The X-ray brightness near 1 keV, obtained in [20] using a radiation source with $\lambda = 3.9$ μm at a peak intensity of 3.3×10^{14} W cm^{-2}, exceeded by four to five orders of magnitude that observed in [21] as a result of expose of helium and neon in gas cells at low (0.5 atm) pressure to light with $\lambda = 0.8$ μm and peak intensity of 2×10^{16} W cm^{-2}.

Progress in implementing generation of short-pulse coherent X rays using HHG of radiation of compact near- and mid-IR sources is important for developing high-time-resolu-

M.Yu. Emelin, M.Yu. Ryabikin Institute of Applied Physics, Russian Academy of Sciences, ul. Ul'yanova 46, 603950 Nizhnii Novgorod, Russia; e-mail: emelin@ufp.appl.sci-nnov.ru, mike@ufp.appl.sci-nnov.ru

Received 4 December 2012
Kvantovaya Elektronika **43** (3) 211–216 (2013)
Translated by Yu.P. Sin'kov

tion spectroscopy in the energy range from several tenths to several units of keV. Wide energy distributions of electrons and photons, obtained in correspondence with (1)–(3) upon ionisation of gases by long-wavelength radiation of relatively low intensity, have some advantages for methods of extracting dynamic structural information about atoms and molecules [22] based on the analysis of HHG and above-threshold ionisation spectra. These are higher spatial resolution, attenuation of some undesirable minor effects, possibility of work with easily ionised materials, etc. [23–25].

The large spectral width of coherent (quasi) supercontinuum, produced at HHG of mid-IR radiation, in principle makes it possible to form pulses with widths from several attoseconds to several tenths of attosecond. An important circumstance is that, according to the semiclassical HHG model, the group-delay dispersion ('attochirp') of high harmonics should decrease with the pump wavelength as $1/\lambda$, which is confirmed by the experimental data of [26]; thus, attochirp can be more easily compensated for in order to shorten attosecond pulses. Concerning the generation of single attosecond pulses, it is important that, when the pump wavelength λ increases, the repetition period of attosecond pulses rises proportionally to λ, while the threshold ellipticity (defined as the laser pump ellipticity at which the harmonic generation efficiency is half the sum of that for linearly polarised pump) decreases as $1/\lambda$ [27]. This leads to less strict requirements to the response speed of polarisation gate [28] for selecting a single pulse and increases its efficiency in the case of mid-IR sources.

Thus, femtosecond mid-IR range sources are of undoubted interest as new promising tools for studies in physics of strong fields and attosecond physics. In this context, it is important to determine their ultimate possibilities in the applications where shorter wavelength sources are widely used and reveal radically new potentialities. Here, these problems are considered as applied to high-harmonic generation.

Phase mismatch of elementary oscillators within a medium (which is related to spatial dispersion) is known to be one of the main factors limiting the spectral width of experimentally observed harmonics. Specifically due to the violation of phase-matching conditions for higher harmonics the width of experimental HHG spectra is often much smaller than that predicted by formula (2) for the high-frequency cutoff energy. Possible ways to solve the phase matching problem in the case of HHG in the mid-IR radiation field were discussed in a number of studies. In this context, we should note different versions of implementing quasi-phase-matching conditions that are widely considered in the literature. These questions are beyond the scope of our study; the corresponding discussions can be found, e.g., in [15, 16].

The emphasis of our study is on the factors limiting the ultimate attainable energies of higher harmonics and their generation efficiency, which are determined by the specific features of the response of elementary atomic oscillators. One of these factors is the influence of the magnetic field of high-intensity laser radiation on the dynamics of free electrons. This influence manifests itself in a deviation of the paths of electrons moving with subrelativistic velocities from straight lines and, as a consequence [29, 30], in a reduced efficiency of high-harmonic generation, which is based on recollisions of electrons with parent ions. When visible or near-IR radiation interacts with neutral atoms, this factor is insignificant, because atoms are ionised at radiation intensities much lower than those at which such relativistic effects may manifest themselves. However, one should expect that, when using long-wavelength sources, this factor may be important even at moderate laser-pulse peak intensities in view of scaling (1).

Another important limiting factor is the depletion of bound levels of working-medium atoms. Since the emission of high-energy photons in the HHG regime under consideration is primarily due to free-bound transitions, the necessary condition for the existence of high-frequency induced polarisation is nonzero population of both free and bound states. In this context, fast depletion of bound levels at laser intensities corresponding to the occurrence of above-barrier ionisation leads to HHG suppression [31, 32]. Joint consideration of the aforementioned factors is important both for determining their relative role during high-harmonic generation under different conditions and for formulating the general conclusions on the limiting possibilities of generating high-energy photons by means of HHG in the mid-IR laser radiation field in gases.

2. Details of numerical calculations

The problem of ionisation of an atom by a femtosecond laser pulse and high-harmonic generation was solved by numerical integration of the time-dependent Schrödinger equation in the single-electron approximation. To study the influence of the laser-pulse magnetic field on the HHG efficiency, we compared the results of the calculations carried out within the electric-dipole approximation and beyond it. In the first case we solved the Schrödinger equation in which the vector potential of the electromagnetic field is assumed to be only time-dependent (hereinafter, we use mainly atomic units):

$$\mathrm{i}\frac{\partial \Psi}{\partial t} = \frac{1}{2}\left[\boldsymbol{p} + \frac{\boldsymbol{A}(t)}{c}\right]^2 \Psi + V(\boldsymbol{r})\,\Psi, \tag{4}$$

where $\boldsymbol{p}$ is the electron momentum operator, c is the speed of light in vacuum, $V(\boldsymbol{r})$ is the interaction potential of electron and parent ion, and $\boldsymbol{A}(t)$ is the laser-field vector potential.

Beyond the framework of the electric-dipole approximation we took into account the smallness of the localisation scale of the electron wave packet in comparison with the laser wavelength and used expansion of the vector potential in spatial coordinates, restricting ourselves to the linear expansion term in the coordinate z (which was chosen to be directed along the propagation direction of laser beam, linearly polarised along the x axis):

$$\boldsymbol{A}(z,t) \approx \boldsymbol{e}_x[A_0(t) + B(t)z] = \boldsymbol{e}_x\left[A_0(t) - \frac{1}{c}\frac{\mathrm{d}A_0}{\mathrm{d}t}z\right].$$

After a unitary transformation the initial equation is reduced to the form [29], which differs from the equation in the electric-dipole approximation by an additional term: $-\mathrm{i}v_z(\partial\Psi/\partial z)$. This term describes the motion of electron along the z axis under the magnetic field of laser radiation. Here, $v_z = (1/2c)\times[A_0(t)/c]^2$ is the z component of the classical electron velocity, calculated in the lower order with respect to v/c.

The laser field was set in the form of a Gaussian pulse with an FWHM equal to six field periods. The laser wavelength was assumed to be 3.9 μm and the intensity was varied in the range from 10^{14} to 2×10^{15} W cm^{-2}.

The nonlinear atomic response to the laser field was calculated using the Ehrenfest theorem, according to which the second derivative of the atomic dipole moment can be found as [33]

$$\ddot{\boldsymbol{d}}(t) = -\frac{\mathrm{d}^2}{\mathrm{d}t^2}\langle \boldsymbol{r} \rangle = \left\langle \Psi(\boldsymbol{r},t) \left| \frac{\partial V(\boldsymbol{r})}{\partial \boldsymbol{r}} + \boldsymbol{E}(t) \right| \Psi(\boldsymbol{r},t) \right\rangle = \boldsymbol{E}(t) + \boldsymbol{R}(t), \quad (5)$$

where

$$\boldsymbol{R}(t) = \int |\Psi(\boldsymbol{r},t)|^2 \frac{\partial V}{\partial \boldsymbol{r}} \mathrm{d}\boldsymbol{r} \quad (6)$$

is the nonlinear part of atomic response. The Schrödinger equation was integrated by the split operator method using fast Fourier transform [34]. The probability for electron to remain in the bound state after the end of the laser pulse was calculated as the norm of the wave function over a region with a size exceeding the Bohr radius by a factor of 100.

To perform correct numerical description of the dynamics of atomic electron in a high-intensity laser field and determine its high-frequency response, a number of conditions must be satisfied. First, since the high-frequency atomic polarisation response is a consequence of interference of the de Broglie waves corresponding to the bound electron and the electron returning to the parent ion under the ac laser field (according to the quantum-mechanical theory of high-harmonic generation in the tunnel-ionisation regime [35]), all parts of the electron wave packet that may return (after leaving the atom) to the small vicinity of the parent ion, should not go beyond the calculation region. This condition limits the sizes of the calculation region from below. Second, the entire wavelength spectrum of the de Broglie waves arising as a result of acceleration of the electron wave packet by the laser pulse field should be resolved well on the coordinate grid. This condition imposes limitations on the maximum allowable grid step in the coordinate space. Third, all frequencies that may arise in the atomic polarisation response as a result of interaction between the atom and the laser field should also be adequately resolved. This condition limits the maximum allowable time step when calculating the evolution of the wave function.

Combination of all these factors results in the following: the computational resources required for calculating the atomic polarisation response in a strong field increase with the laser wavelength as λ^5. If HHG in radiation fields of a Ti:sapphire laser or some other visible or near-IR source is simulated, three-dimensional quantum-mechanical calculations can be fairly easily implemented. However, when passing to mid-IR sources, the calculation time and number of computation steps become so large that three-dimensional calculations can hardly be performed. In this context, we restrict ourselves to numerical calculations within the two-dimensional model. The approach based on the use of low-dimensionality models is widely applied in problems of the physics of strong fields (see [36] and references therein). Numerous examples described in the literature prove adequacy (at least qualitative) of this approach as applied to processes occurring in strong fields, if the set of coordinates used for simulation includes all coordinates that are of fundamental importance for the physical problem under study. In our case such physically important coordinates are those describing the motion of a classical electron in the plane formed by the electric field direction and the wave vector of the incident electromagnetic wave (hereinafter, coordinates x and y, respectively).

We use a two-dimensional model in which the interaction potential of the electron and parent ion is set by the expression

$$V(\boldsymbol{r}) \equiv V(x,y) = -\frac{Z}{\sqrt{a^2 + x^2 + y^2}}, \quad (7)$$

where Z is the effective charge of the atomic nucleus and a is the smoothing parameter of Coulomb singularity. The calculations were performed for $a = 0.8$ and $Z = 1$ and 2. Model potential (7) is a two-dimensional generalisation [37] of the smoothed Coulomb potential proposed in [38]. In a certain sense, taking into account the asymptotics of potential (7) at $r \to \infty$, one can say that the model set by this potential is a two-dimensional analogue of hydrogen atom and singly charged helium ion at $Z = 1$ and 2, respectively. Moreover, at $Z = 1$ and a chosen value of the smoothing parameter, the ground-state energy in potential (7) is equal to the ionisation potential of hydrogen atom ($I_\mathrm{i} \approx 13.6$ eV).

However, we should note the following: it is of fundamental importance to describe adequately the ionisation probability of atoms in order to solve the problem stated. It is known [36] that low-dimensionality models yield much higher ionisation rates than their three-dimensional analogues for the same I_i value. Our study showed that, as applied to neutral atoms of noble gases, model (7) describes most adequately (with regard to the ionisation rate) xenon and helium at $Z = 1$ and 2, respectively. In the more general form, one can state that the two cases considered in this study correspond to atoms with low (at $Z = 1$) and high (at $Z = 2$) ionisation potentials.

3. Calculation results

The results of numerical calculations are presented in Figs 1–4.

Figures 1 and 2 show the nonlinear polarisation response spectra calculated for model atoms with $Z = 1$ and $Z = 2$ at different laser-pulse peak intensities. The spectra presented in Figs 1a and 2a correspond to peak intensities much lower than the ionisation saturation intensity. There are hardly any signs of depletion of bound levels in these cases; the spectra have a smooth plateau-like profile with a pronounced cutoff at energies that are well consistent with classical expression (2). The cutoff is followed by a sharp drop (by seven to eight orders of magnitude) of the nonlinear response spectral intensity.

Note that in the case $Z = 1$, even at a relatively low pulse peak intensity (10^{14} W cm^{-2}), the large part of the plateau-like distribution (cutoff energy of about 465 eV) falls in the range that is important for many applications: the so-called water window (282.1–530.4 eV). When $Z = 2$ (a case corresponding to an atom with an ionisation potential exceeding that for $Z = 1$ by a factor of about 2.5), at an intensity of 6×10^{14} W cm^{-2}, which only slightly exceeds the ionisation threshold (at this intensity the ionisation probability during the entire pulse is less than 0.25%), the high-frequency plateau edge is located at about 2.7 keV (which corresponds to a wavelength 0.46 nm). Concerning the influence of the magnetic field at the aforementioned intensities, it is practically absent for $Z = 1$, whereas for $Z = 2$ it suppresses harmonic generation by a factor of more than 3.

The change in the role of the effects limiting the harmonic generation efficiency for the model atoms under consider-

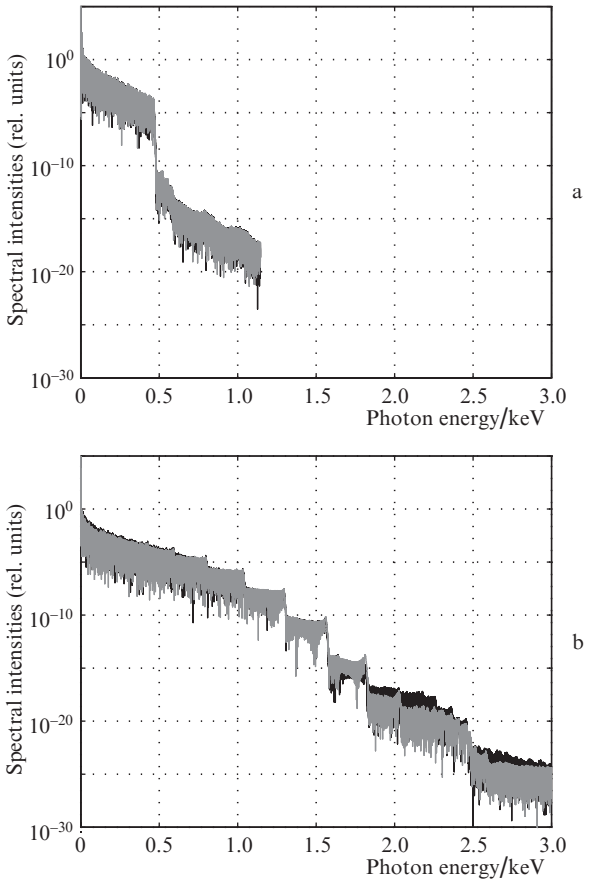

Figure 1. Spectra of nonlinear polarisation response for a model atom with $Z = 1$. The peak intensity of a laser pulse with a centre wavelength of 3.9 μm and a width of 78 fs is (a) 10^{14} and (b) 5×10^{14} W cm^{-2}. The spectra calculated disregarding and taking into account the laser pulse magnetic field are shown by black and grey, respectively.

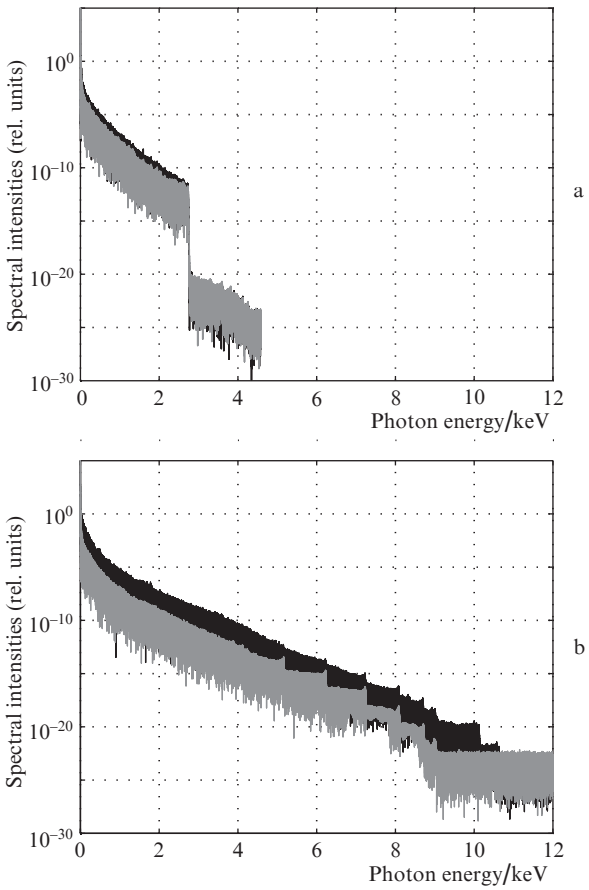

Figure 2. The same as in Fig.1 but for a model atom with $Z = 2$ at laser-pulse peak intensities of (a) 6×10^{14} and (b) 2×10^{15} W cm^{-2}.

ation with an increase in the pulse peak intensity is clearly illustrated by Figs 3 and 4.

Figure 3 shows the calculated (for a model atom with $Z = 1$) dependences on the laser-pulse peak intensity for the following parameters: the total intensity W of nonlinear polarisation response in the energy range above the low-frequency boundary of the water window (282.1 eV), calculated disregarding ($W^{(d)}$) and taking into account ($W^{(nd)}$) the laser-pulse magnetic field, the ratio $W^{(nd)}/W^{(d)}$, and the bound-state population after the end of the pulse.

It can be seen that in the case $Z = 1$ the maximum level of high-harmonic suppression induced by the magnetic field is only about 30%; however, even this effect can hardly be observed, because it arises at laser intensities at which the bound-state population decreases by more than three orders of magnitude. Thus, the depletion of bound levels for $Z = 1$ is the main factor limiting the high-harmonic generation. The character of its influence on the harmonic spectrum can be seen well in Fig. 1b. In this case, the spectrum is a set of short plateau-like portions with cutoffs at energies equal to the maximum energies of electrons returning to the parent ion during the corresponding half-periods of laser-pulse electric field oscillations. At photon energies above 1 keV, the yield of harmonics between neighbouring plateau-like portions drops by three orders of magnitude. This drop is due to the sharp increase in the ionisation rate when passing through the laser pulse front; it confirms the well-known fact that, under the ionisation saturation conditions, the time interval corresponding to the most efficient harmonic generation shifts to earlier times with respect to the pulse envelope peak with an increase in the pulse intensity.

The dependences calculated for the model atom with $Z = 2$ (Fig.4) are similar to those shown in Fig. 3. The W value was calculated as the total intensity of the nonlinear polarisation response in the energy range above 1.24 keV, which corresponds to wavelengths shorter than 1 nm.

The results presented in Fig. 4 differ significantly from the data on $Z = 1$. With the magnetic field neglected, the higher-harmonic generation efficiency is maximum at a peak intensity of 1.2×10^{15} W cm^{-2}. Due to the effect of the magnetic field, the optimal intensity is reduced to 10^{15} W cm^{-2}; in this case, higher harmonics are suppressed by a factor of about 10. It should be noted that the decrease in the bound-state population is only about 10%; i.e., the effect of the magnetic field is pronounced and plays a key role. At higher intensities the relative role of bound-state depletion increases. At intensities of about 1.5×10^{15} W cm^{-2} each of these two factors reduces the harmonic yield near the high-frequency cutoff by more than an order of magnitude; the cutoff energy is about 7 keV, which corresponds to a wavelength of about 0.18 nm. At even higher intensities the factor of bound-state depletion becomes dominant. For example, in the high-frequency region of the spectrum in Fig. 2b, which was calculated for a peak intensity $I = 2 \times$

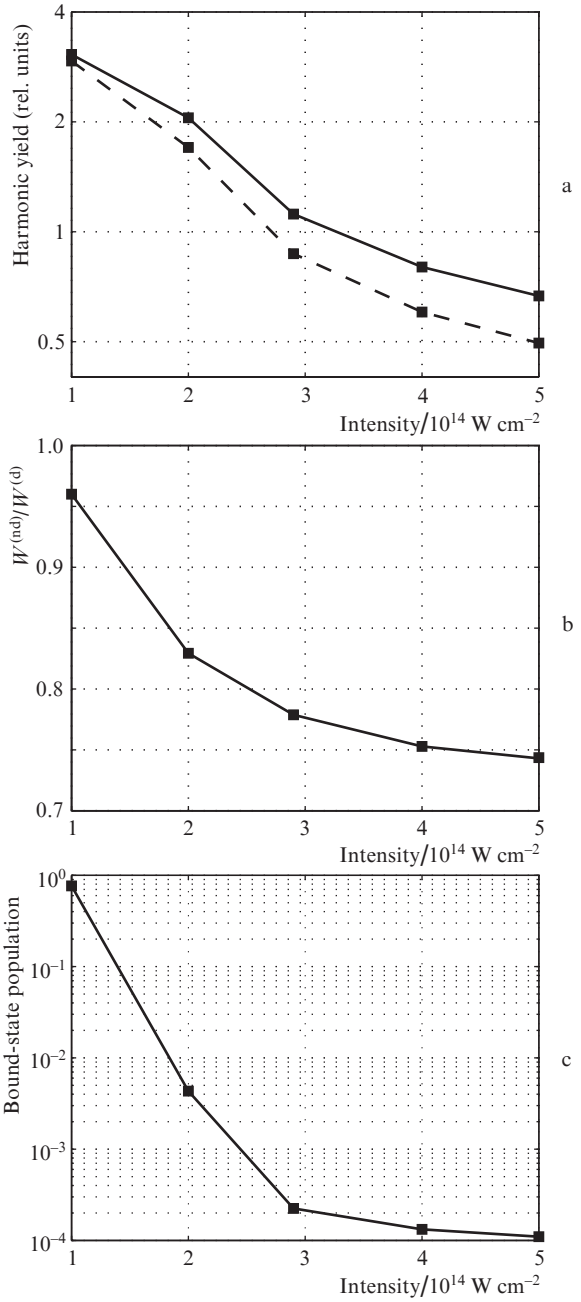

Figure 3. A model atom with $Z = 1$. Calculated dependences on the laser-pulse peak intensity: (a) the total nonlinear response intensity in the energy range above the low-frequency boundary of the water window [the solid and dashed curves correspond to the integral harmonic yields calculated disregarding ($W^{(d)}$)) and taking into account ($W^{(nd)}$)) the laser-pulse magnetic field], (b) the $W^{(nd)}/W^{(d)}$ratio, and (c) the bound-state population after the end of the pulse.

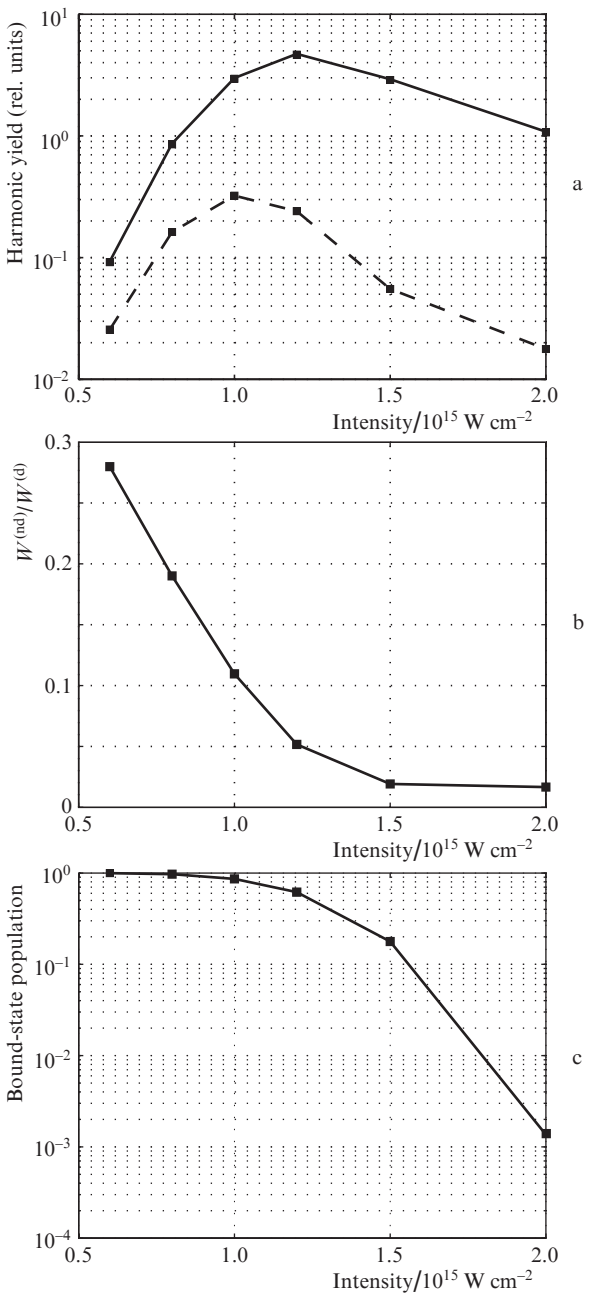

Figure 4. The same as in Fig. 3 but for a model atom with $Z = 2$. The total nonlinear response intensity corresponds to the energy range of harmonics with wavelengths less than 1 nm.

10^{15} W cm^{-2}, one can clearly see several short plateau-like portions; the drop of harmonic yield between each pair of neighbouring portions is approximately an order of magnitude.

4. Conclusions

The results of our numerical calculations make it possible to reveal the role of the factors related to the influence of laser-pulse magnetic field and depletion of bound levels of working-medium atoms in the case of HHG of mid-IR laser radiation in gases. The relative role of these factors is determined to a great extent by the ionisation potential of the atoms of the medium. Under irradiation of atoms with a low (below 12 eV) ionisation potential by high-intensity femtosecond pulses with a centre wavelength of 3.9 μm, one should expect generation of harmonics with energies to about 1 keV; in this case, the main limiting factor is the bound-state depletion. Irradiation of atoms with a high (above 20 eV) ionisation potential is expected to yield much higher harmonics with wavelengths less than 2Å. Here, the laser radiation magnetic field is the main factor of harmonic suppression in a wide range of laser-pulse peak intensities. The latter circumstance is of independent interest for experimental observation of relativistic effects using desktop mid-IR lasers.

Acknowledgements. This work was supported by the Presidium of the Russian Academy of Sciences (programme 'Extreme Light Fields and Their Applications'), the Russian Foundation for Basic Research (Grant Nos 12-02-12101-ofi_m, 10-02-01250, and 12-02-31325), Federal Target Programme 'Personnel' (Agreement No. 8729/01.10.2012), and grant NSh-5430.2012.2 of the President of the Russian Federation for Support of Leading Scientific Schools. M.Yu. Emelin acknowledges the non-profit Dynasty Foundation for support. We are grateful to the administrations of the Interdepartmental Supercomputer Centre of the Russian Academy of Sciences and SNIC for supplying computational resources.

References

1. Vozzi C., Calegari F., Benedetti E., Gasilov S., Sansone G., Cerullo G., Nisoli M., De Silvestri S., Stagira S. *Opt. Lett*., **32**, 2957 (2007).
2. Gu X., Marcus G., Deng Y., et al. *Opt. Express*, **17**, 62 (2009).
3. Hauri C.P., Lopez-Martens R.B., Blaga C.I., et al. *Opt. Lett*., **32**, 868 (2007).
4. Schmidt B.E., Béjot P., et al. *Appl. Phys. Lett*., **96**, 121109 (2010).
5. Andriukaitis G., Balciunas T., et al. *Opt. Lett*., **36**, 2755 (2011).
6. Deng Y., Schwarz A., Fattahi H., et al. *Opt. Lett*., **37**, 4973 (2012).
7. Vozzi C., Negro M., Stagira S. *J. Mod. Opt*., **59**, 1283 (2012).
8. McPherson A., Gibson G., et al. *J. Opt. Soc. Am. B*, **4**, 595 (1987).
9. Ferray M., L'Huillier A., Li X.F., Lompre L.A., Mainfray G., Manus C. *J. Phys. B: At. Mol. Opt. Phys*., **21**, L31 (1988).
10. Krause J.L., Schafer K.J., Kulander K.C. *Phys. Rev. Lett*., **68**, 3535 (1992).
11. Corkum P.B. *Phys. Rev. Lett*., **71**, 1994 (1993).
12. Yang B., Schafer K.J., et al. *Phys. Rev. Lett*., **71**, 3770 (1993).
13. Paulus G.G., Becker W., Nicklich W., Walther H. *J. Phys. B: At. Mol. Opt. Phys*., **27**, L703 (1994).
14. Shan B., Chang Z. *Phys. Rev. A*, **65**, 011804(R) (2001).
15. Yakovlev V.S., Ivanov M., Krausz F. *Opt. Express*, **15**, 15351 (2007).
16. Popmintchev T., Chen M.-C., Bahabad A., Gerrity M., Sidorenko P., Cohen O., et al. *Proc. Natl Acad. Sci. USA*, **106**, 10516 (2009).
17. Tate J., Auguste T., Muller H.G., Salières P., Agostini P., DiMauro L.F. *Phys. Rev. Lett*., **98**, 013901 (2007).
18. Colosimo P., Doumy G., Blaga C.I., et al. *Nature Phys*., **4**, 386 (2008).
19. Shiner A.D., Trallero-Herrero C., et al. *Phys. Rev. Lett*., **103**, 073902 (2009).
20. Popmintchev T., Chen M.-C., Popmintchev D., Arpin P., Brown S., Ališauskas S., Andriukaitis G., et al. *Science*, **336**, 1287 (2012).
21. Seres E., Seres J., Spielmann C. *Appl. Phys. Lett*., **89**, 181919 (2006).
22. Lein M. *J. Phys. B: At. Mol. Opt. Phys*., **40**, R135 (2007).
23. Peters M., Nguyen-Dang T.T., Cornaggia C., Saugout S., Charron E., Keller A., Atabek O. *Phys. Rev. A*, **83**, 051403(R) (2011).
24. Vozzi C., Negro M., Calegari F., Sansone G., Nisoli M., De Silvestri S., Stagira S. *Nature Phys*., **7**, 822 (2011).
25. Torres R., Siegel T., Brugnera L., et al. *Opt. Express*, **18**, 3174 (2010).
26. Doumy G., Wheeler J., Roedig C., Chirla R., Agostini P., DiMauro L.F. *Phys. Rev. Lett*., **102**, 093902 (2009).
27. Strelkov V.V., Khokhlova M.A., Gonoskov A.A., Gonoskov I.A., Ryabikin M.Yu. *Phys. Rev. A*, **86**, 013404 (2012).
28. Platonenko V.T., Strelkov V.V. *Kvantovaya Elektron*., **25**, 771 (1998) [*Quantum Electron*., **28**, 749 (1998)].
29. Kim A.V., Ryabikin M.Yu., Sergeev A.M. *Usp. Fiz. Nauk*, **169**, 58 (1999).
30. Walser M.W., Keitel C.H., Scrinzi A., Brabec T. *Phys. Rev. Lett*., **85**, 5082 (2000).
31. Moreno P., Plaja L., Malyshev V., Roso L. *Phys. Rev. A*, **51**, 4746 (1995).
32. Strelkov V.V., Sterjantov A.F., Shubin N.Yu., Platonenko V.T. *J. Phys. B: At. Mol. Opt. Phys*., **39**, 577 (2006).
33. Burnett K., Reed V.C., Cooper J., Knight P.L. *Phys. Rev. A*, **45**, 3347 (1992).
34. Fleck J.A. Jr., Morris J.R., Feit M.D. *Appl. Phys*., **10**, 129 (1976).
35. Lewenstein M., Balcou Ph., Ivanov M.Yu., L'Huillier A., Corkum P.B. *Phys. Rev. A*, **49**, 2117 (1994).
36. Silaev A.A., Ryabikin M.Yu., Vvedenskii N.V. *Phys. Rev. A*, **82**, 033416 (2010).
37. Babin A.A., Kim A.V., Kiselev A.M., Sergeev A.M., Stepanov A.N. *Izv. Vyssh. Uchebn. Zaved., Ser. Radiofiz*., **39**, 713 (1996).
38. Javanainen J., Eberly J.H., Su Q. *Phys. Rev. A*, **38**, 3430 (1988).